Journal of Power Sources 239 (2013) 513–526

Contents lists available at SciVerse ScienceDirect

Journal of Power Sources

journal homepage: www.elsevier.com/locate/jpowsour

Optimal planning of Molten Carbonate Fuel Cell Power Plants at distribution networks considering Combined Heat, Power and Hydrogen production

Taher Niknam [a], Mosayeb Bornapour [a], Amir Ostadi [b,*], Amirhossein Gheisari [c]

[a] Department of Electrical and Electronic Engineering, Shiraz University of Technology, Shiraz, Iran
[b] University of Waterloo, Canada
[c] Islamic Azad University, Fars Science and Research Branch, Iran

HIGHLIGHTS

- Propose a stochastic model for planning the location and operation of Molten Carbonate Fuel Cell Power Plants (MCFCPPs).
- Consider the effect of Combined Heat, Power, and Hydrogen (CHPH) simultaneously.
- Manage generation of thermal energy, and hydrogen, total emission of MCFCPPs and network.
- Consider uncertainties of the pressures of input hydrogen, oxygen, and carbon dioxide importing to MCFCPP.

ARTICLE INFO

Article history:
Received 11 November 2012
Received in revised form
1 March 2013
Accepted 20 March 2013
Available online 3 April 2013

Keywords:
Molten Carbonate Fuel Cell Power Plants (MCFCPPs)
Combined Heat, Power, and Hydrogen (CHPH)
2m+1 Point Estimate Method (2m+1 PEM)
Self Adaptive Learning Bat-inspired Algorithm (SALBA)
Pareto optimal set

ABSTRACT

In this paper, a stochastic model is used for optimal planning of Molten Carbonate Fuel Cell Power Plants (MCFCPPs) in distribution network for producing Combined Heat, Power, and Hydrogen (CHPH). Total production costs of electrical energy, thermal energy, and hydrogen, emissions of MCFCPPs and network, and voltage deviation are considered in the objective function. In this paper, location and operation of MCFCPPs are taken into consideration while their investment cost is not taken into account. In this model, the uncertainties in forecasting the electrical and thermal loads, the pressures of hydrogen, oxygen, and carbon dioxide, and the indeterminacy of the nominal temperature of MCFCPP are considered using 2m + 1 Point Estimate Method (2m + 1 PEM). The problem of optimal planning of MCFCPPs as CHPH is of mixed integer nonlinear nature. So, a Self Adaptive Learning Bat-inspired Algorithm (SALBA) is employed for solving this problem. The problem is solved as a multi-objective one to achieve the best Pareto optimal set. A set of non-dominated solutions are saved in a repository and the proposed method is evaluated on a 69-bus distribution system.

1. Introduction

Power system deregulation encourages electrical companies to employ renewable energy resources [1]. Renewable energies could properly substitute the fossil fuels and noticeably reduce green house gases [2]. Molten Carbonate Fuel Cell Power Plant (MCFCPP) is a profitable renewable energy resource in which electro–chemical reaction between hydrogen and oxygen produces electricity, heat, and water [3], [4]. MCFCPPs have no rotating part, produce ignorable acoustic noise, and benefit from environment-friendly power production [5], [6]. They operate at high temperatures and are proper options for being used as CHPH [7]. In addition, as hydrogen is produced from methane, there is no need for direct sources of hydrogen [8].

Recently, many studies have addressed the operation of Distributed Generations (DGs) and renewable energy resources in distribution networks. Effects of DG locations on voltage stability margin in distribution networks are investigated in Ref. [9]. Moravej and Akhlaghi investigated the impacts of positioning of DGs on voltage profile improvements and power loss reductions using a novel approach based on cuckoo search [10]. Biswas et al. proposed a new formulation

* Corresponding author.
E-mail addresses: niknam@sutech.ac.ir (T. Niknam), mbornapour@yahoo.com (M. Bornapour), amir.ostadi@gmail.com (A. Ostadi), amirhossein.gheisari@yahoo.com (A. Gheisari).

0378-7753/$ – see front matter © 2013 Published by Elsevier B.V.
http://dx.doi.org/10.1016/j.jpowsour.2013.03.117

Nomenclature

V_{MCFCPP} output voltage of MCFCPP
E_{eq} equivalent cell potential
R universal gas constant (8.3145 kJ kmol^{-1} K^{-1})
z number of electrons transferred per molecule of fuel
P_{H_2} pressure of hydrogen gas
P_{O_2} pressure of oxygen gas
P_{H_2O} pressure of water vapor
$P_{CO_{2,c}}$ pressure of carbon dioxide gas in cathode
$P_{CO_{2,a}}$ pressure of carbon dioxide gas in anode
Temp MCFCPP temperature
i_{MCFCPP} output current of MCFCPP
$-\Delta\overline{g}_f$ change in Gibbs free energy of the hydrogen reaction
F Faraday constant
R_{ohmic} ohmic cell resistance
$\eta_{cathode}$ the re-scaled cathodic over-potential
η_{anode} the re-scaled anodic over-potential
A active area cell
I_{max} maximum current density
P_{MCFCPP} output active power of MCFCPP
X decision variable
t_{max} total time
P^t_{Sub} active power produced by the substation of network
C_{Sub} cost of substation active power
C_{n1} price of purchasing natural gas for FCPPs
N_{FCPP} total number of FCPPs
P^t_{FCPPj} active power generated by MCFCPPj during time t
$P^t_{H_{FCPPj}}$ equivalent electric power for hydrogen production during time t
$\eta^t_{MCFCPP,j}$ efficiency of MCFCPPj during time t
C_{n2} fuel price for thermal loads
N_{bus} total number of buses
L_{thi} thermal load demand of bus i
P^t_{thi} heat produced by MCFCPP in bus i if there is a FCPP in this bus during time t
OM operation and maintenance costs of FCPPs
C_{pump} hydrogen pumping cost
$P_{H_{FCPPUsage}}$ equivalent electrical energy of used hydrogen
C_{Hs} hydrogen selling price
$P_{H_{Save,FCPP}}$ equivalent electrical energy of saved hydrogen
H_{factor} a conversion factor (kg of hydrogen/kW of electric power), where $H_{factor} = 1.05 \times 10^{-8}/v_{cell}$ and v_{cell} is the cell operating voltage, $v_{cell} = 0.6$ V.
h number of objective function
$locat_n$ the location of MCFCPP$_n$
$N_\mu(X_i)$ normalized membership value of each particle in the repository
d number of non-dominated solutions in the repository
T total time
E^t_{grid} emission produced by grid during time t
$E^t_{FCPP,j}$ emission produced by MCFCPPj units during time t
e_{grid,SO_2} emission coefficient of grid
e_{grid,NO_x} emission coefficient of grid
e_{grid,CO_2} emission coefficient of grid
e_{MCFCPP,SO_2} emission coefficient of MCFCPP units
e_{MCFCPP,NO_x} emission coefficient of MCFCPP units
e_{MCFCPP,CO_2} emission coefficient of MCFCPP units
V_{ref} nominal voltage
V^t_i voltage magnitude of the bus i during time t
V_{Min} lowest voltages of each bus
V_{Max} highest voltages of each bus
$P^{t,min}_{MCFCPP,j}$ the minimum of active power produced by MCFCPPj during time t
$P^{t,max}_{MCFCPP,j}$ the maximum of active power produced by MCFCPPj during time t
Δt step time
$P_{Max,MCFCPP}$ the maximum power of MCFCPP
r_{TEj} the thermal energy to electrical energy ratio
f^{min}_i the lower bound of each objective function
f^{max}_i the upper bound of each objective function
$\mu_{fi(x)}$ membership function of each objective function
$Iter_{max}$ maximum number of iterations
Iter current iteration
A^k_m, r^k_m Pulse loudness and emission rate for the mth bat in iteration k, respectively.
A^k_{mean} Mean of the pulse loudness for all bats in iteration k.
$\mathbf{Gbest}^k$ Best compromise solution in iteration k.
f_m Pulse frequency of the mth bat.
f^{min}_m, f^{max}_m Minimum and maximum pulse frequency for bat m, respectively.
$\mathbf{Mean}^k$ Mean of the population positions.
$\mathbf{Pbest}^k_m$ Best position for bat m in iteration k.
$\mathbf{Worst}^k$ The worst solution among all bats in iteration k.
N_{Bat} Number of bats
$\mathbf{Vel}^k_{new,j}, \mathbf{Vel}^k_j$ new and old velocities of the jth bat, respectively
$\mathbf{X}^k_{new,j}, \mathbf{X}^k_j$ new and old positions of the jth bat, respectively.
rand(.) random number between 0 and 1
w_k weight of kth objective function
η_{st} hydrogen storage efficiency
$\eta^t_{overall}$ overall efficiency of MCFCPP

List of abbreviations

MCFCPP Molten Carbonate Fuel Cell Power Plants
CHPH Combined Heat, Power, and Hydrogen
SALBA Self Adaptive Learning Bat-inspired Algorithm
DG Distributed Generation
RWM Roulette Wheel Mechanism
MCS Monte Carlo Simulation
SD Standard Deviation
CF Constant Frequency
FM Frequently Modulated
SALM Self Adaptive Learning Mechanism
PEM 2m + 1 Point Estimate Method
PDF Probability Distribution Function
DLF Deterministic Load Flow
MOP Multi-objective Optimization Problem

for placement of DGs using a combination of technical factors such as power loss minimization and voltage sag reduction and economical factors such as costs of maintenance and mount of DGs in the system [11]. Optimal placement and sizing of DGs using a multi-objective methodology are offered in Ref. [12]. El-Zonkoly studied the optimal positioning of new resources of energy in distribution networks considering different load models [13]. In Refs. [14], optimal placement and sizing of DGs are addressed based on fuel cost minimization, power loss reduction, and voltage profile improvement using a novel efficient population-based heuristic approach. Moradi and Abedini studied the problem of optimal placement and sizing of FCPPs using a combination of PSO and GA algorithms [15]. Niknam et al. formulated the optimal positioning of renewable energy sources in distribution networks in a Multi-objective Optimization Problem and used a modified honey bee mating optimization algorithm to obtain the solutions [16]. For location and size

determination of DGs, Jabr and Pal proposed an ordinal optimization method to do a trade-off between loss minimization and DG capacity maximization [17]. Alrashidi and Alhajri approached the problem of optimal placement and sizing of DGs based on power loss reduction using an improved PSO algorithm [18]. Wang et al. determined the locations of DGs and drove the optimal re-closer in radial distribution networks using ant colony optimization algorithm [19]. Reference [20] determined the locations of DGs using load flow analysis based on determination of sensitive buses to voltage collapse. In Refs. [21,22], modeling and operation of MCFCPPs were addressed in detail. In Refs. [23], Niknam et al. investigated the operation management of micro grids considering electrical and thermal power production of fuel cells. Gravitational Search algorithm and Point Estimate Method were used for solving the optimization problem. El-Sharkh et al. investigated different models for operational cost of fuel cells as CHPH [24,25]. Positioning and operation of fuel cells as CHPH were determined using a fuzzy adaptive modified particle swarm optimization [26]. In Refs. [27], design and operation of fuel cells as CHP were investigated for supplying residential loads. The study proved high efficiency of fuel cells as CHP power units. In Refs. [28], a solar PV-electrolyzer system and a fuel cell were coupled for supplying electrical and thermal loads. In this work, hydrogen was obtained from electrolysis of water and stored in a storage tank. Reference [29] discussed the combination of a micro gas turbine and a fuel cell in supplying electrical and thermal loads. In this paper, biogas was used as the main energy source of the system.

In the previous papers, operation and optimal placement of MCFCPPs have not been simultaneously planned and the inherent uncertainties of electrical and thermal load forecasting and input gases of MCFCPPs have not been considered. The Monte Carlo Simulation (MCS) approach is a straightforward method for dealing with the uncertainties. However, it is significantly time consuming [30]. In this paper, 2m + 1 PEM as a simple and flexible approach is employed for modeling the uncertainties of electrical and thermal loads, operational temperature of MCFCPPs, and pressures of input oxygen, hydrogen, and carbon dioxide importing to MCFCPPs [31,32]. Normal Probability Distribution Function (PDF) is used to model the variations of uncertainty parameters.

In this paper, optimal placement and sizing of MCFCPPs as CHPH in distribution networks are addressed. Various factors such as uncertainties of electrical and thermal load forecasting, pressures of hydrogen, oxygen, and carbon dioxide and temperature of MCFCPPs are considered. The problem of optimal placement and sizing of MCFCPPs as CHPH is a mixed integer nonlinear problem. An evolutionary algorithm called Self Adaptive Learning Bat-inspired Algorithm (SALBA) is employed to solve this optimization problem [33].

The rest of the paper is organized as follows: Section 2 deals with modeling of MCFCPPs in steady state conditions. In Section 3, the problem of optimal placement and sizing of MCFCPPs as CHPH in distribution networks is formulated. Thermal energy and hydrogen production strategies are discussed in Sections 4 and 5, respectively. Section 6 addresses the 2m + 1 PEM formulation. In Sections 7 and 8, Multi-objective approach of Pareto optimal solutions and Best compromise solutions are discussed. Formulation of the Self-Adaptive Learning Bat-Inspired Algorithm (SALBA) is provided in Section 9. Section 10 addresses the implementation of SALBA for optimal placement and operation of MCFCPPs in distribution networks. Simulation results are given in Section 11 and finally, Section 12 concludes the paper.

2. Steady state model of MCFCPPs

In fuel cells, oxidation and reduction reactions in anode and cathode, respectively creates a voltage at the terminals of the fuel cell stack. Following these reactions, electrical energy and heat are produced. Fig. 1 represents the basic characteristic of an MCFCPP and the half-cell reactions in the anode and cathode electrodes.

2.1. Half-cell reactions

The combination of hydrogen and carbonate ions produces water and carbon dioxide and releases electrons. These electrons are transferred to the cathode through an external circuit. In addition to the main reduction reaction, it is very likely to have a water-gas shift reaction in presence of CO.

Anode reaction:

$$\begin{aligned} &2H_2 + 2CO_3^{2-} \rightarrow 2H_2O + 2CO_2 + 4e^- \\ &CO + H_2O \rightarrow CO_2 + H_2 \quad (\text{water} - \text{gas shift reaction}) \end{aligned} \tag{1}$$

Cathode reaction:

$$O_2 + 2CO_2 + 4e^- \rightarrow 2CO_3^{2-}, \tag{2}$$

The overall reaction is:

$$\frac{1}{2}O_2 + H_2 \rightarrow H_2O \tag{3}$$

The carbonate ions of the cathode go to the anode through the electrolyte. In contrast to alkaline fuel cell and proton exchange membrane fuel cell, CO_2 is the major component in cathode reaction. Oxygen (either pure or in the form of air) reacts with CO_2 yields carbonate ions. Two methods can be used for transferring CO_2 to cathode electrode: (i) using a CO_2 permeable membrane and (ii) using an external recirculation of the anode exhaust after complete combustion process. At the anode, hydrogen can be generated from steam-reforming process of natural gas. Another way is to directly provide hydrogen from electrolysis of water. Methane as the main energy carrier of the natural gas reacts with water at the presence of a catalyst (usually nickel) to produce the required hydrogen. To enhance efficiency of the system, the waste heat of the MCFCPPs is used in this reaction resulting in an endothermic process. The reaction in steam reforming process is:

$$CH_4 + H_2O \rightarrow CO + 3H_2 \tag{4}$$

Besides, water-gas shift reaction occurs in the reformer. The exhaust gas consists of a combination of CO, CO_2, and H_2O.

2.2. Open-circuit voltage

Performance of an MCFCPP is usually monitored using its voltage characteristics versus current density (polarization curve).

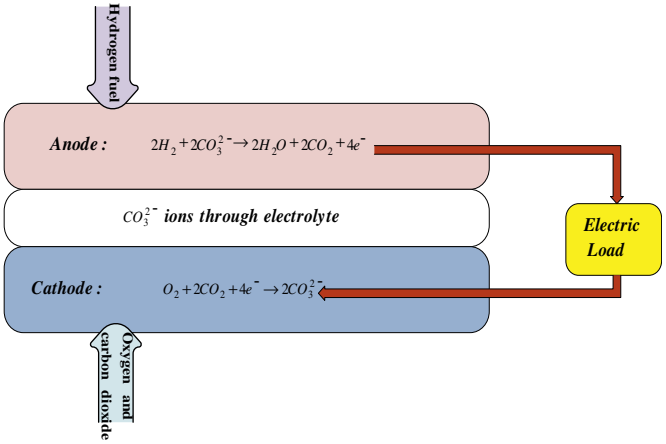

Fig. 1. Operation principle of the MCFCPP.

The polarization profile of MCFCPPs depends on their operating conditions such as the utilization amount of reactant gases and their compositions. Assuming that the fuel cell is in a thermodynamic equilibrium state, its open-circuit voltage is identical to its reversible potential. The Nernst equation in (5) expresses the relationship between the equilibrium cell potential (E_{eq}) and the standard cell potential (E^0) in an MCFCPP:

$$E_{eq}(\text{Temp}, P_i) = E^0(\text{Temp}, P) + \frac{R \times \text{Temp}}{zF} \ln\left\{ \left[\frac{P_{H_2} P_{O_2}^{1/2}}{P_{H_2O}} \right] \left[\frac{P_{CO_2,c}}{P_{CO_2,a}} \right] \right\} \quad (5)$$

where '*a*' and '*c*' represent the anode and cathode, respectively. The value of E_{eq}(Temp,P_i) equals the cell potential at partial pressures P_i (atm) and temperature Temp. $E^0(T,P)$ is the reversible cell voltage of the MCFCPP at $P_i = 1$ atm and 650 °C and can be calculated via [34]:

$$E^0 = -\Delta\bar{g}_f / zF \quad (6)$$

where '*z*' corresponds to the number of electrons transferred for each reacting molecule of hydrogen in the fuel cell, '*F*' represents the Faraday constant and '$-\Delta\bar{g}_f$' is the change in Gibbs free energy in the hydrogen reaction with oxygen (H_2 + (1/2) O_2 → H_2O). Using these data, the reversible cell voltage is calculated to be:

$$E^0 = \frac{197000}{2 \times 96485} V = 1.02\ V \quad (\text{at } 650\ ^\circ\text{C and } 1\ \text{atm}) \quad (7)$$

2.3. Current density and cell potential

Equations (8) and (9) show the relation between the cell current (I) and the molar amount of oxygen and carbon dioxide utilized in the cell reactions, respectively [21,34]:

$$\text{molar}O_2\ \text{usage} = I/4F \quad (8)$$

$$\text{molar}CO_2\ \text{usage} = I/2F \quad (9)$$

As it is more common to use the current density of MCFCPP in the cell equations, the electrical power can be determined by (considering identical dynamics for each of the cells):

$$\text{stack power} = \text{cell voltage} \times i \times \text{active surface area} \times \text{number of cell} \quad (10)$$

where i is the average current density. Defining the cell voltage in Equation (10) as V_{MCFCPP}, one has:

$$V_{MCFCPP} = E_{eq} - i(R_{ohmic} + \eta_{anode} + \eta_{cathode}) \quad (11)$$

where $E_{eq} = 1.02$ V; R_{ohmic} represents the ohmic cell resistance and can be determined by Ref.[35]:

$$R_{ohmic} = 0.5 \times 10^{-4} \times \exp\left[3016\left(\frac{1}{\text{Temp}} - \frac{1}{923}\right)\right] \quad (12)$$

In Equation (11), η_{anode} and $\eta_{cathode}$ correspond to the re-scaled anodic and cathodic over-potentials which can be experimentally estimated using [35]:

$$\eta_{anode} = 2.27 \times 10^{-9} \times \exp\left(\frac{6435}{\text{Temp}}\right) \times P_{H_2}^{-0.42} \times P_{CO_2}^{-0.17} \times P_{H_2O}^{-1.0} \quad (13)$$

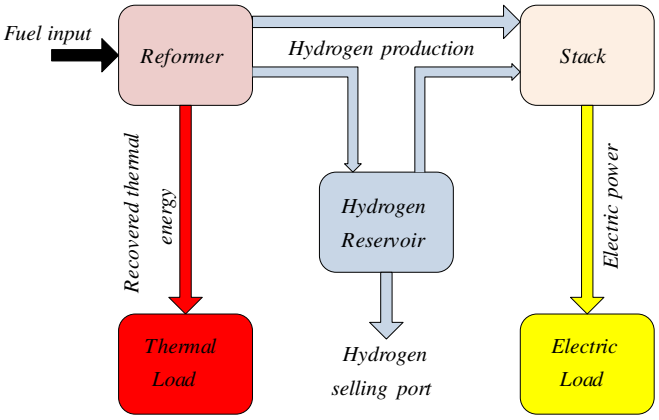

Fig. 2. Schematic operation flow chart of MCFCPP employed as CHPH.

$$\eta_{cathode} = 7.505 \times 10^{-10} \times \exp\left(\frac{9298}{Temp}\right) \times P_{O_2}^{-0.43} \times P_{CO_2}^{-0.09} \quad (14)$$

where P_i demonstrates the partial pressure of species '*i*' at the inlet. Equations (13) and (14) are valid only for operation temperatures in the range of 600–700 °C [36]. Assuming the unity power factor, the output active power of fuel cell is determined as:

$$P_{MCFCPP} = i_{MCFCPP} \times V_{MCFCPP} \quad (15)$$

3. Optimal placement and operation of MCFCPPs in distribution networks

In this paper, optimal positioning and operation of MCFCPPs are determined by solving a nonlinear optimization problem with several conflicting objectives as follows:

3.1. Objective function

3.1.1. Decision variables

Various decision variables are defined for formulating the optimization problem as:

$$X = \left[L_{MCFCPP} \quad i_{MCFCPP} \quad P_{H_{MCFCPP}} \quad P_{H_{MCFCPPUsage}} \right]_{1 \times n \times (1+3T)} \quad (16)$$

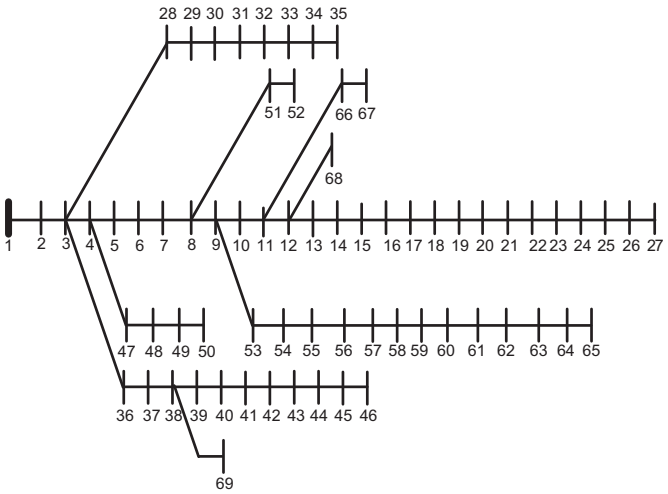

Fig. 3. Single line diagram of distribution test system.

$$L_{\mathrm{MCFCPP}} = [\mathrm{locat}_1 \quad \mathrm{locat}_2 \quad \ldots \quad \mathrm{locat}_n]_{1\times n} \tag{17}$$

$$i_{\mathrm{MCFCPP}} = \left[i_{\mathrm{MCFCPP}_1} \quad i_{\mathrm{MCFCPP}_2} \quad \cdots \quad i_{\mathrm{MCFCPP}_n} \right]_{1\times n\times T} \tag{18}$$

$$i_{\mathrm{MCFCPP}j} = \left[i^1_{\mathrm{MCFCPP}j} \quad i^2_{\mathrm{MCFCPP}j} \quad \cdots \quad i^t_{\mathrm{MCFCPP}j} \quad \cdots \quad i^T_{\mathrm{MCFCPP}j} \right]_{1\times T} \tag{19}$$

$$P_{H_{\mathrm{MCFCPP}}} = \left[P_{H_{\mathrm{MCFCPP1}}} \quad P_{H_{\mathrm{MCFCPP2}}} \quad \cdots \quad P_{H_{\mathrm{MCFCPPn}}} \right]_{1\times n\times T} \tag{20}$$

$$P_{H_{\mathrm{MCFCPP}j}} = \left[P^1_{H_{\mathrm{MCFCPP}j}} \quad P^2_{H_{\mathrm{MCFCPP}j}} \quad \cdots \quad P^t_{H_{\mathrm{MCFCPP}j}} \quad \cdots \quad P^T_{H_{\mathrm{MCFCPP}j}} \right]_{1\times T} \tag{21}$$

$$P_{H_{\mathrm{MCFCPPUsage}}} = \left[P_{H_{\mathrm{MCFCPPUsage},1}} \quad P_{H_{\mathrm{MCFCPPUsage},2}} \quad \cdots \quad P_{H_{\mathrm{MCFCPPUsage},n}} \right]_{1\times n\times T} \tag{22}$$

$$P_{H_{\mathrm{MCFCPPUsage},j}} = \left[P^1_{H_{\mathrm{MCFCPPUsage},j}} \quad P^2_{H_{\mathrm{MCFCPPUsage},j}} \quad \cdots \quad P^t_{H_{\mathrm{MCFCPPUsage},j}} \quad \cdots \quad P^T_{H_{\mathrm{MCFCPPUsage},j}} \right]_{1\times T} \tag{23}$$

3.1.2. Operation cost

One of the elements of the objective function in this paper is the operation cost which includes different terms such as costs of output electrical and thermal energy of the MCFCPPs, electrical energy of the substation, and the hydrogen production by MCFCPPs. If thermal energy produced by MCFCPPs does not meet the required thermal load, natural gas is used for supplying it. The cost function is formulated as [24,25]:

$$\begin{aligned} f_1(X) = \sum_{t=1}^{T} \Bigg(& P^t_{\mathrm{Sub}} \times C_{\mathrm{Sub}} + C_{n1} \sum_{j}^{N_{\mathrm{MCFCPP}}} \left(\frac{P^t_{MCFCPPj} + P^t_{H_{MCFCPPj}}}{\eta^t_{MCFCPP,j}} \right) \\ & + C_{n2} \sum_{i}^{N_{bus}} \max(L_{thi} - P^t_{thi}, 0) + OM \\ & + C_{pump} \sum_{j}^{N_{MCFCPP}} \eta_{st} \times \left(P^t_{H_{\mathrm{MCFCPP}j}} + P^t_{H_{\mathrm{MCFCPPUsage}\,j}} \right) \\ & - C_{Hs} \sum_{j}^{N_{\mathrm{MCFCPP}}} \left(P^t_{H_{\mathrm{Save,MCFCPP}j}} \times H_{\mathrm{factor}} \right) \Bigg) \end{aligned} \tag{24}$$

Different terms of the operation cost function are:

- Cost of electrical energy produced by the substation.
- Cost of requisite fuel of the MCFCPPs.
- Cost of required natural gas.
- Cost of operation and maintenance of the MCFCPPs.
- Cost of pumping the hydrogen to MCFCPPs or storage.
- Income of hydrogen selling at the end of the day.

3.1.3. Emission

Concerns about environmental pollution of MCFCPPs and substations encourages considering an emission-based term in the objective function as follows [26]:

Table 1
MCFCPP nominal parameters in detail.

N	48
Temp	923 K
A	62.5 cm^2
P_{H_2}	1.467 atm
P_{O_2}	0.2095 atm
P_{CO_2}	1 atm
P_{H_2O}	1 atm
$I_{\max}$	0.7 A

$$f_2(X) = \sum_{t=1}^{T} \left(E^t_{\mathrm{grid}} + \sum_{j=1}^{N_{\mathrm{MCFCPP}}} E^t_{\mathrm{MCFCPP},j} \right) \tag{25}$$

$$E^t_{\mathrm{grid}} = P^t_{\mathrm{Sub}} \times e_{\mathrm{grid},SO_2} + P^t_{\mathrm{Sub}} \times e_{\mathrm{grid},NO_x} + P^t_{\mathrm{Sub}} \times e_{\mathrm{grid},CO_2} \tag{26}$$

$$E^t_{\mathrm{MCFCPP}j} = P^t_{\mathrm{MCFCPP}j} \times e_{\mathrm{MCFCPP},SO_2} + P^t_{\mathrm{MCFCPP}j} \times e_{\mathrm{MCFCPP},NO_x} + P^t_{\mathrm{MCFCPP}j} \times e_{\mathrm{MCFCPP},CO_2} \tag{27}$$

3.1.4. Voltage deviation

Minimizing the voltage deviations noticeably enhances power quality. In this paper, a term based on the level of voltage deviation is considered in the objective function by [26]:

$$f_3(X) = \frac{\sum_{t=1}^{T} \sum_{i=1}^{N_{\mathrm{bus}}} \left(\frac{\left| V_{\mathrm{ref}} - V^t_i \right|}{V_{\mathrm{ref}}} \right) \times \Delta t}{N_{\mathrm{Bus}}} \tag{28}$$

3.2. Constraints

- Limits of bus voltages

$$V_{\mathrm{Min}} \le |V^t_i| \le V_{\mathrm{Max}} \tag{29}$$

- Active power outputs of MCFCPPs

$$P^{t,\min}_{\mathrm{MCFCPP},j} \le P^t_{\mathrm{MCFCPP},j} \le P^{t,\max}_{\mathrm{MCFCPP},j} \tag{30}$$

- Magnitude of the current of MCFCPPs

$$I^{\min}_{\mathrm{MCFCPP}} \le I^t_{\mathrm{MCFCPP}} \le I^{\max}_{\mathrm{MCFCPP}} \tag{31}$$

- Equivalent electric power of the produced hydrogen

Table 2
Determinant parameters information of cost objective function.

Parameter	Value
Cost of substation active power, C_{Sub} ($ kwh^{-1})	0.035
Price of natural gas for MCFCPPs, C_{n1} ($ kwh^{-1})	0.04
Fuel price for thermal loads, C_{n2} ($ kwh^{-1})	0.05
Operation and maintenance cost of MCFCPPs, OM ($ h^{-1})	19.32
Hydrogen selling price, C_{Hs} ($ kg^{-1})	1.8
Hydrogen pumping cost, C_{pump} ($ kwh^{-1})	0.01
Hydrogen storage efficiency, η_{st}	95%

$$0 \le P^t_{H_{\mathrm{MCFCPP}}} \le 250 - P^t_{\mathrm{MCFCPP}} \tag{32}$$

- Equivalent electric power of the utilized hydrogen

$$0 \le P^t_{H_{\mathrm{MCFCPPUsage}}} \le \max\left\{(250 - P^t_{\mathrm{MCFCPP}}), \sum_{k=1}^{t-1}\left(P^t_{H_{\mathrm{MCFCPP}}} - P^t_{H_{\mathrm{MCFCPPUsage}}}\right)\right\} \tag{33}$$

4. Thermal energy production strategy

In order to enhance the efficiency of MCFCPPs, one practical approach is to utilize the heat produced by the MCFCPPs. In this paper, electrical efficiency and the ratio of heat to electrical energy of the MCFCPPs in every operating time interval are considered to be $\eta^t_{\mathrm{MCFCPP},j} = 0.5013$ and $r_{\mathrm{TE}j} = 1.0067452$, respectively [37]. Thermal energy produced by the MCFCPPs is a function of their output electrical energy and is determined as [26]:

$$P^t_{\mathrm{thi}} = r_{\mathrm{TE}j} \times \left(P^t_{\mathrm{MCFCPP}j} + P^t_{Hj}\right) \tag{34}$$

$$P_{\mathrm{Max,MCFCPP}} = P^t_{\mathrm{MCFCPP}j} + P^t_{Hj} \tag{35}$$

Without considering MCFCPPs as CHPH, their efficiency is approximately in the range of 40–48%. Employing MCFCPPs as CHPH noticeably improves their efficiency. The overall efficiency of MCFCPPs is defined by [24]:

$$\eta^t_{\mathrm{overall}} = \frac{P^t_{\mathrm{MCFCPP}} + \eta_{\mathrm{st}} \times P^t_{H_{\mathrm{MCFCPP}}} + \min(P^t_{\mathrm{th}}, L^t_{\mathrm{th}})}{\frac{P^t_{\mathrm{MCFCPP}} + P^t_{H_{\mathrm{MCFCPP}}}}{\eta^t_{\mathrm{MCFCPP}j}}} \tag{36}$$

5. Hydrogen production strategy

The principle goal of hydrogen production is to utilize full capacity of the MCFCPPs when their electrical energy production is less than their nominal capacities. To implement this strategy, the remaining capacity of the MCFCPP is modeled by an equivalent amount of electrical energy. The hydrogen production varies between zero and the difference between the actual output power of MCFCPP and its nominal capacity. Using this strategy, MCFCPP chooses between consuming or storing hydrogen in the most optimum way.

Fig. 2 is a flow chart of operation of an MCFCPP employed as CHPH. Since the reactions are exothermic, the plant thermal energy could be recovered for supplying thermal loads and the produced hydrogen goes to the stack. A portion of produced hydrogen is used for electricity production and the rest goes to the hydrogen reservoir for future usages or selling at the end of the day.

6. 2m + 1 PEM

Presence of random variables in distribution systems necessitates considering uncertainty when dealing with problems in this regard. Thus, conventional tools which need deterministic data are not accurate enough to be applied. Several articles have addressed the probabilistic techniques which handle the uncertainties related to problems in power systems [31].

6.1. Formulation of 2m + 1 PEM

6.1.1. Location and weight factor

Let us define $\mathbf{Z} = [z_1, z_2, ..., z_n]'$ as a set of nonlinear multi-variant equations shown in Equation (37). This set represents the power flow equations. By solving these equations using statistical knowledge of $\mathbf{Z}$, statistical information of the input variables $\boldsymbol{p}$ is achieved. The output variable $\mathbf{Z}$ corresponds to the steady state operating conditions of the power system.

$$\mathbf{Z} = \mathbf{F}(p_1, p_2, ..., p_m) \tag{37}$$

where z_i represents the ith output variable and p_l shows the lth input variable. The 2m + 1 PEM is a numerical method in which a random probability distribution function evaluated at three points is assigned to each input variable ($P_{l,k}$) along with three corresponding weighting factors ($w_{l,k}$) where $l = 1,2,\ldots,m$ and $k = 1,2,3$. Now, the function $\mathbf{F}$ is evaluated at each point, and the corresponding weighting factor determines the impact on the characteristics of the output variables. The first four central moments of each random input variable including Mean, Variance, and coefficients of Skewness and Kurtosis are used in 2m + 1 PEM for determining the location and weighting factors as follows:

$$p_{l,k} = \mu_{p_l} + \xi_{l,k}\sigma_{p_l} \quad k = 1,2,3 \& l = 1,2,\ldots,m \tag{38}$$

In which $\xi_{l,k}$ is the standard location and μ_{pl} and σ_{pl} represent the Mean and Standard Deviation (SD) of the input variable p_l, respectively. The values of the standard locations are determined by:

$$\xi_{l,k} = \frac{\lambda_{p_l,3}}{2} + (-1)^{3-k}\sqrt{\lambda_{p_l,4} - \frac{3}{4}\lambda^2_{p_l,3}} \quad k = 1,2 \quad ,\xi_{l,3} = 0 \tag{39}$$

The variables $\lambda_{pl,3}$ and $\lambda_{pl,4}$ represent the coefficients of Skewness and Kurtosis of the variable p_l, respectively. Generally, the ith central moment of the variable p_l is determined as follows:

$$\lambda_{l,i} = \frac{E\left[\left(p_l - \mu_{p_l}\right)^i\right]}{\left(\sigma_{p_l}\right)^i} \tag{40}$$

As mentioned before, each location, $p_{l,k}$ corresponds to a weighting factor $w_{l,k}$, which is determined by:

$$w_{l,k} = \frac{(-1)^{3-k}}{\xi_{l,k}(\xi_{l,1} - \xi_{l,2})} k = 1,2, \quad w_{l,3} = \frac{1}{m} - \frac{1}{\lambda_{p_l,4} - \lambda^2_{p_l,3}} \tag{41}$$

Once the location and weight factor are determined, the values of Mean and SD of the output variables will be computed.

6.1.2. Mean and Standard Deviation of the output variables

In order to compute the Mean and SD of each output variable, the function $\mathbf{F}$ is evaluated at the corresponding pair of ($P_{l,k}$,$w_{l,k}$) with the other input variables substituted by their Mean values. This is formulated as:

$$Z_i(l,k) = F_i\left(\mu_{p_1}, \mu_{p_2}, ..., \mu_{p_{l-1}}, p_{l,k}, \mu_{p_{l+1}}, ...\mu_{p_m}\right) \tag{42}$$

After calculation of Z for all random input variables, the value of the jth moment of the random output variable is determined using:

$$E\left(z_i^j\right) = \sum_{l=1}^{m}\sum_{k=1}^{3} w_{l,k}(z_i(l,k))^j \tag{43}$$

When $j = 1$, it corresponds to the Mean value for the ith random output variable. The SD is computed as by:

$$\mu_{z_i} = E(z_i)$$
$$\sigma_{z_i} = \sqrt{E\left(z_i^2\right) - (E(z_i))^2} = \sqrt{E\left(z_i^2\right) - \mu_{z_i}^2} \quad (44)$$

7. Multi-objective approach of Pareto optimal solutions

In a Multi-objective Optimization Problem (MOP), there is more than a single objective function and usually there is no optimal solution which simultaneously optimizes all objective functions. In this case, decision makers desire to have the most preferred solution [38]. Generally, MOP can be mathematically explained as:

$$\text{Find the vector } X = [x_1, x_2, ..., x_n] \text{ to optimize}$$
$$F(X) = [f_1(X), f_2(X), ..., f_K(X)]^T_{(1\times K)} \quad (45)$$

Subject to

$$g_i(X) \le 0, \quad i = 1, 2, ..., N_{ieq} \quad (46)$$

$$h_j(X) = 0, \quad j = 1, 2, ..., N_{eq} \quad (47)$$

In an MOP, efficiency or Pareto optimality replaces the concept of optimality. An efficient (non-dominated, Pareto optimal, non-inferior) solution is the one which cannot improve one objective function without reducing the optimality of at least one of the other objective functions. This can be explained as follows:

$\mathbf{X}^*$ is the Pareto optimal solution in the search space of χ if:

$$\forall k \in \{1, 2, 3, ..., K\} : \forall X \in \chi - \left\{X^*\right\}, f_k\left(X^*\right) \le f_k(X) \& \exists m \in \{1, 2, 3, ..., K\} : f_m\left(X^*\right) < f_m(X) \quad (48)$$

8. Best compromise solution

It is essential to choose a solution among the non-dominated solutions of the Pareto optimal set as the best compromise solution. Since the objective functions mentioned before are not precise, they are considered to be fuzzy sets. In this procedure, a fuzzy membership function is selected for determining the best compromise solution. For all the particles of the repository, a membership function is determined for each objective function as follows [16]:

$$\mu_{f_i(X)} = \begin{cases} 0 & ,f_i(X) \ge f_i^{\max} \\ \dfrac{f_i^{\max} - f_i(X)}{f_i^{\max} - f_i^{\min}} & ,f_i^{\min} \le f_i(X) \le f_i^{\max} \\ 1 & ,f_i(X) \le f_i^{\min} \end{cases} \quad (49)$$

where $f_i^{\max}$ and $f_i^{\min}$ represent the upper and lower bounds of each objective function, respectively. For evaluation of these values, they are compared with the results achieved by optimization of each objective function independently.

The normalized membership values of the particles of the repository could be determined as follows [16]:

$$N_\mu(X_i) = \frac{\sum_{k=1}^{h} w_k \times \mu_{fk}(X_i)}{\sum_{i}^{d}\sum_{k}^{h} w_k \times \mu_{fk}(X_i)} \quad (50)$$

where h represents the number of objective functions, d is the number of non-dominated solutions of the repository, and w_k represents the weight of kth objective function. The best compromise solution is the one of which N_μ is maximum.

9. Self-Adaptive Learning Bat-Inspired Algorithm (SALBA)

9.1. Original bat-inspired algorithm

Echolocation or bio sonar is the biological sonar employed by several kinds of animals. Echolocating animals send some signals to their surroundings environment and receive their returning echos for locating and identifying objects. Echolocation is also used in various domains for navigating and foraging. In 18th century, an Italian scientist, Lazzaro Spallanzani had shown that bats navigate by hearing power, not by vision power. Bats produce echolocation calls in terms of pitch with both Constant Frequency (CF calls) and variant frequency which are Frequently Modulated (FM calls). Although low frequently acoustic signals travel further than high-frequently ones, high frequently calls give bats more detailed information of preys such as range, speed, size, position, and the direction of prey flight. BA is a novel population-based evolutionary algorithm which is inspired from food foraging of bats. The echolocation of bat can be employed for optimizing multi-objective problems. The bat algorithm is based on following assumptions [39]:

- Each bat uses the echolocation system for determining the differences of prey and obstacles.
- In order to find a prey, each bat at position $\mathbf{X}_m^k$ with velocity $\mathbf{Vel}_m^k$ flies randomly and emits signals with loudness A_m^k and frequency f_m.
- They can automatically adjust the frequency of their produced pulse and tune pulse emission rate of r_m^k.
- The loudness value of A_m^k can change in different ways such as decreasing from large values to small values.

As demonstrated in Section 3$\mathbf{X}_m^k$, $\mathbf{Vel}_m^k$, and $\mathbf{Pbest}_m^k$ represent position, velocity, and the best position matrices of each bat m at iteration k respectively. They are defined as:

$$\mathbf{X}_m^k = [\mathbf{X}_{m,1}^k \quad \mathbf{X}_{m,2}^k \quad ... \quad \mathbf{X}_{m,n\times(1+3T)}^k] \quad (51)$$

$$\mathbf{Vel}_m^k = [\mathbf{Vel}_{m,1}^k \quad \mathbf{Vel}_{m,2}^k \quad ... \quad \mathbf{Vel}_{m,n\times(1+3T)}^k] \quad (52)$$

$$\mathbf{Pbest}_m^k = [\mathbf{Pbest}_{m,1}^k \quad \mathbf{Pbest}_{m,2}^k \quad ... \quad \mathbf{Pbest}_{m,n\times(1+3T)}^k] \quad (53)$$

Furthermore, a fitness value is devoted to each bat m:

$$F(\mathbf{X}_m^k) = \max_{q=1,2}\left[\mu_{F_q}^{ref} - \mu_{F_q}(\mathbf{X}_m^k)\right] \quad (54)$$

Every bat remembers its best position as $\mathbf{Pbest}_m^k$ in each iteration. The position of the best compromise solution is represented by $\mathbf{Gbest}^k$. The bats modify these velocities and positions for finding the optimal solution. The position and velocity of each particle are updated using following equations [33]:

$$\mathbf{Vel}_m^{k+1} = \mathbf{Vel}_m^k + f_m\left(\mathbf{Gbest}^k - \mathbf{X}_m^k\right) m = 1, ..., N_{\text{Bat}} \quad (55)$$

$$\mathbf{X}_m^{k+1} = \mathbf{X}_m^k + \mathbf{Vel}_m^{k+1} \quad m = 1, ..., N_{\text{Bat}} \quad (56)$$

$$f_m = f_m^{\min} + \text{rand}(.)\left(f_m^{\max} - f_m^{\min}\right) \quad m = 1, ..., N_{\text{Bat}} \quad (57)$$

After this movement, for each bat, a new solution is locally produced using random walk and the below procedure is followed for generating the new solution:

If $\text{rand}(.) > r_m^k$

A local solution is generated around $\mathbf{Pbest}_m^k$ as follows [33]:

$$\mathbf{X}_{m,\text{new}}^{k+1} = \mathbf{X}_m^{k+1} + \varepsilon A_{\text{mean}}^k(\mathbf{Pbest}_m^k - \mathbf{X}_m^k) m = 1,\ldots,N_{\text{Bat}} \quad (58)$$

Else

A local solution is generated around the randomly chosen solution $r_1 \neq m$ as follows:

$$\mathbf{X}_{m,\text{new}}^{k+1} = \mathbf{X}_m^{k+1} + \varepsilon A_{\text{mean}}^k(\mathbf{X}_{r_1}^k - \mathbf{X}_m^k) m = 1,\ldots,N_{\text{Bat}} \quad (59)$$

End

If $\left(\text{rand}(.) < A_m^k\right) \wedge (F(\mathbf{X}_{m,\text{new}}^{k+1}) < F(\mathbf{X}_{m,\text{new}}^k)$

The new solution of the mth bat is accepted as the initial population of the next iteration. It should be considered that A_i^k and r_i^k are updated according to the following relation [33]:

$$A_i^{k+1} = \alpha A_i^k; r_i^{k+1} = r_i^1(1 - \exp(-\gamma(k+1))) \quad (60)$$

End

In which γ and α are constant parameters. The best position of each bat and that of all the bats i.e. $\mathbf{Pbest}_m^k$ and $\mathbf{Gbest}^k$ are updated in this step.

It is obvious that the dynamic of the proposed algorithm is like that of a Particle Swarm Optimization (PSO) [26], but the loudness and pulse rate of BA make it operate like the combination of standard PSO and an intensive local search which is similar to Simulated Annealing (SA) [40] methods for local searching.

In comparison with the other evolutionary methods, BA has many noticeable advantages in solving complex nonlinear optimization problems such as placement and operation of MCFCPPs as CHPH. Easy implementation, simple concepts, high stability, and low execution efforts are some of its benefits. In contrast, it often converges to improper solutions because of local optima existence, lack of bat diversity, or algorithm slow proceeding which would be eliminated as explained later.

9.2. Self Adaptive Learning Mechanism (SALM)

SALBA is a framework by which the robustness and performance of BA is improved for obtaining good results from numerical optimization problem with different characteristic. Its main idea is selection of multiple effective strategies based on their prior experiences of generating promising solution and applying them for achieving the mutation operation. It means that multiple strategies would be assigned in different steps of optimization procedure based on their success rate in generating enhanced solutions within specific number of previous generation. In this paper, four mutation strategies are employed in SALBA for diversing complex placement and operation of MCFCPPs as CHPH problem. These mutation operators can be explained as follows:

Table 3
Emission coefficients related to NO_x, SO_2 and CO_2.

Emission coefficients (gr kwh^{-1})		
Emission type	Substation	MCFCPP
NO_x	2.29518	0.0001361
SO_2	3.58337	0.0104326
CO_2	921.245352	421.84056

Mutation strategy 1:

$$\mathbf{X}_{m,1}^k = \mathbf{X}_m^k + \text{round}(1 + \text{rand}(.))\left(\mathbf{Gbest}^k - \mathbf{Mean}^k\right) \quad m = 1,\ldots,N_1^k \quad (61)$$

Mutation strategy 2:

$$\mathbf{X}_{m,2}^k = \mathbf{X}_{r_1}^k + \text{rand}(.)_1\left(\mathbf{Gbest}^k - \mathbf{Worst}^k\right) \quad m = 1,\ldots,N_2^k \quad (62)$$

Mutation strategy 3:

$$\mathbf{X}_{m,3}^k = \mathbf{X}_{r_1}^k + \text{rand}(.)_1(\mathbf{X}_{r_2}^k - \mathbf{X}_{r_3}^k) + \text{rand}(.)_2(\mathbf{X}_{r_4}^k - \mathbf{X}_{r_5}^k) \quad m = 1,\ldots,N_3^k \quad (63)$$

Mutation strategy 4:

$$\mathbf{X}_{m,4}^k = \left(\frac{\mathbf{X}_{r_1}^k + \mathbf{X}_{r_2}^k + \mathbf{X}_{r_3}^k}{3}\right) + (R_1 - R_2)(\mathbf{X}_{r_2}^k - \mathbf{X}_{r_1}^k) + (R_3 - R_2)(\mathbf{X}_{r_2}^k - \mathbf{X}_{r_3}^k) + (R_1 - R_3)(\mathbf{X}_{r_3}^k - \mathbf{X}_{r_1}^k) \quad m = 1,\ldots,N_4^k \quad (64)$$

where $R' = |F(\mathbf{X}_{r_1}^k)| + |F(\mathbf{X}_{r_2}^k)| + |F(\mathbf{X}_{r_3}^k)|$, $R_1 = |F(\mathbf{X}_{r_1}^k)|/R', R_2 = |F(\mathbf{X}_{r_2}^k)|/R'$, and $R_3 = |F(\mathbf{X}_{r_3}^k)|/R'$. N_1^k, N_2^k, N_3^k and N_4^k are the number of bats in iteration k which choose the mutation methods 1, 2, 3, and 4 respectively. In this regard, the vectors $\mathbf{X}_{r_1}^k \mathbf{X}_{r_2}^k \mathbf{X}_{r_3}^k$, $\mathbf{X}_{r_4}^k$ and $\mathbf{X}_{r_5}^k$ are randomly chosen from the existing population in order to cover the algorithm search domain uniformly. This operation could be implemented for all the target vectors in each of the mutation strategies. In order to enhance the solutions of the proposed large-scale problem, improve the population diversity, and ameliorate the global search capabilities, the mutation methods Equations (58)–(61) can be employed.

Generally, having different characteristics and strengths to cover various conditions is the criterion of choosing these four strategies. Mutation occurrence is one of the requirements of BA searching process. All bats of the population have chance of mutation according to the probability of employed methods for mutating. So, each particle chooses one of these four methods according to a probability model. The initial probability of employing ath mutation strategy is considered to be $\text{Prob}_a^1 = 0.25, a = 1,2,3,4$. The Roulette Wheel Mechanism (RWM) is used to choose ath method for each bat of the population. Prob_a^k is updated after LP iterations based on following equation:

$$\text{Prob}_a^k = \frac{SR_a^k}{\sum_{a=1}^4 SR_a^k}; a = 1,\ldots,4 \quad (65)$$

where, SR_a^k shows the success rate of the trial solutions produced by ath mutation strategy which have successfully entered the next step within the previous LP in kth iteration. Thus, SR_a^k could be formulated according to the following equation:

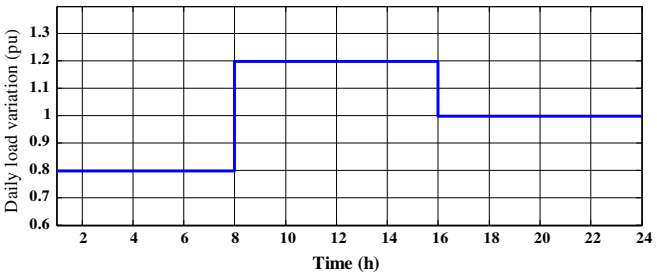

Fig. 4. Daily load variation.

Table 1
Simulation results of multi-objective deterministic problem for different strategies.

		Strategy 1			Strategy 2			Strategy 3		
		Base load	Up load	Low load	Base load	Up load	Low load	Base load	Up load	Low load
Location	$MCFCPP_1$		61						63	
	$MCFCPP_2$		27						22	
	$MCFCPP_3$		66						16	
	$MCFCPP_4$		17						20	
P_{MCFCPP}(Kw)	$MCFCPP_1$	1.7072×10^3	1.6828×10^3	746.7666	174.1716	733.3728	187.7754	1.7072×10^3	1.7072×10^3	1.592×10^3
	$MCFCPP_2$	1.6328×10^3	1.7072×10^3	1.6165×10^3	173.2556	1.5357×10^3	1.4808×10^3	2.448	2.448	1.7072×10^3
	$MCFCPP_3$	1.6559×10^3	206.4151	2.448	86.9099	1.5914×10^3	1.5086×10^3	1.7072×10^3	2.448	88.3159
	$MCFCPP_4$	15.9525	1.5075×10^3	1.6471×10^3	1.5646×10^3	1.4699×10^3	1.544×10^3	1.7072×10^3	1.7072×10^3	221.2935
P_{th}(Kw)	$MCFCPP_1$	1.7187×10^3	1.6942×10^3	751.8037	2.0135×10^3	2.0135×10^3	$2.0135^* \times 10^3$	1.8484×10^3	1.9121×10^3	1.7118×10^3
	$MCFCPP_2$	1.6438×10^3	1.7187×10^3	1.6274×10^3	2.0135×10^3	2.0135×10^3	2.0135×10^3	1.3746×10^3	1.7697×10^3	1.7692×10^3
	$MCFCPP_3$	1.6671×10^3	207.8074	2.4645	2.0135×10^3	2.0135×10^3	2.0135×10^3	1.8614×10^3	1.5461×10^3	1.7924×10^3
	$MCFCPP_4$	16.0601	1.5177×10^3	1.6582×10^3	2.0135×10^3	2.0135×10^3	2.0135×10^3	1.7734×10^3	2.0084×10^3	1.0352×10^3
$P_{H_{MCFCPP}}$(Kw)	$MCFCPP_1$	0	0	0	1.8258×10^3	1.2666×10^3	1.8122×10^3	128.8392	192.0447	108.2677
	$MCFCPP_2$	0	0	0	1.8267×10^3	464.2716	519.2342	1.363×10^3	1.7554×10^3	50.1755
	$MCFCPP_3$	0	0	0	1.9131×10^3	408.6085	491.4055	141.7275	1.5333×10^3	1.6921×10^3
	$MCFCPP_4$	0	0	0	435.3888	530.1239	456.0373	54.315	287.7069	806.9591
$P_{H_{MCFCPPUsage}}$ (Kw)	$MCFCPP_1$	0	0	0	1.8258×10^3	1.2666×10^3	1.8122×10^3	29.8098	101.8798	282.5889
	$MCFCPP_2$	0	0	0	1.8267×10^3	464.2716	519.2342	286.7949	1.061×10^3	292.7878
	$MCFCPP_3$	0	0	0	1.9131×10^3	408.6085	491.4055	94.8142	49.9955	1.2589×10^3
	$MCFCPP_4$	0	0	0	435.3888	530.1239	456.0373	51.5992	70.5762	975.4653
$P_{H_{Save,MCFCPP}}$ (Kw)	$MCFCPP_1$		0			0		14.8731		
	$MCFCPP_2$		0			0		1.5279×10^3		
	$MCFCPP_3$		0			0		1.9634×10^3		
	$MCFCPP_4$		0			0		51.3403		
Cost ($)		7.4192×10^3			7.8252×10^3			7.7523×10^3		
Emission (gr)		8.1533×10^7			7.5605×10^7			8.0081×10^7		
Voltage Deviation (pu)		0.4822			0.419			0.4497		

$$SR_a^k = \frac{\sum_{it=k-LP}^{k-1} ns_a^{it}}{\sum_{it=k-LP}^{k-1}\left(ns_a^{it} + nf_a^{it}\right)} + \delta; a = 1, ..., 4; k > LP \quad (66)$$

where, ns_a^{it} is the number of the trial solutions generated by ath mutation strategy which remain in selection procedure during the previous LP iteration and nf_a^{it} represts the ones which fail. To avoid possible null values of SR_a^k, the constant δ is added to the equation and it is considered to equal 0.01. Using Equation (62) ensure that the sum of the possibilities of chosen strategies equals one. It could be inferred that the higher the value of SR_a^k, the more the probability of employing it for generating the trial solutions at iteration k. To this end, RWM is used to select ath mutation strategy for every bat.

10. SALBA implementation for optimal placement and operation of MCFCPPs

The procedure of the SALBA can be summarized as following steps:

Step 1: Considering all required data.

Step 2: Determining the location and weighting factor of 2m + 1 PEM as follows:

Step 2–1: modeling all sources of uncertainty individually using a normal PDF with related mean value and an SD equal to 5% of the corresponding mean value.

Step 2–2: Generating samples (1000 samples) for each source of uncertainty corresponding to its PDF and calculating $\lambda_{l,3}$ and $\lambda_{l,4}$ using Equation (38).

Step 2–3: Computing the location and weight factors using first four central moments.

Step 2–4: Preparing 2m + 1 points in form of$(\mu_{p'_1}, \mu_{p'_2}, ..., \mu_{p'_{l-1}}, p'_{l,k}, \mu_{p'_{l+1}}, ...\mu_{p'_m})$.

Now, these points convert probabilistic load flow to the deterministic ones.

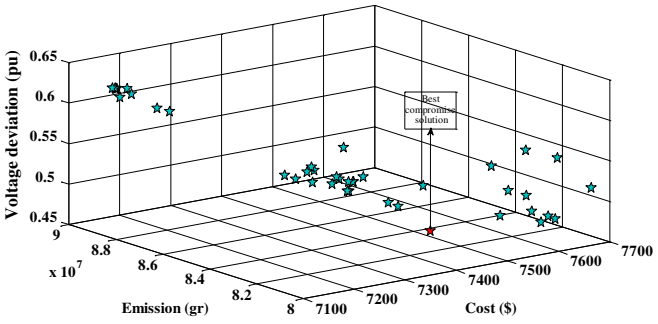

Fig. 5. Pareto front for objective functions considering strategy 1 and a deterministic problem.

Step 3: Generating the initial population: in this paper an initial population is used based on the chaos initialization as follows:

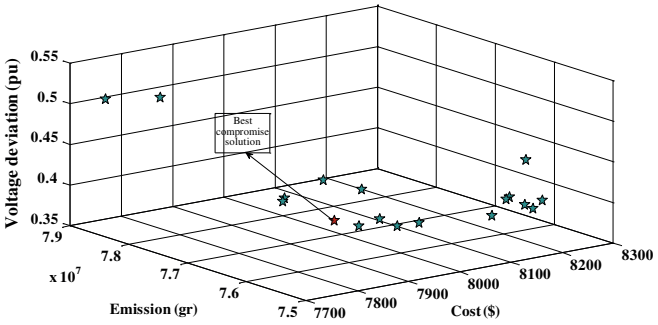

Fig. 6. Pareto front for objective functions considering strategy 2 and a deterministic problem.

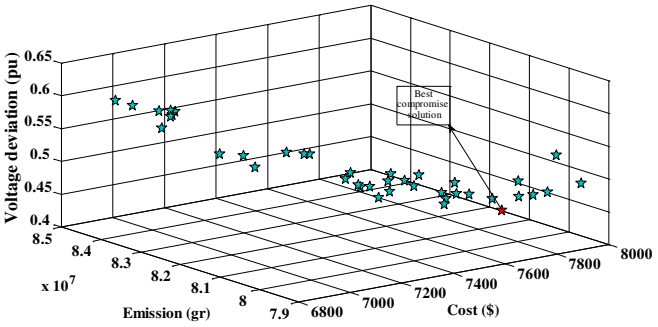

Fig. 7. Pareto front for objective functions considering strategy 3 and a deterministic problem.

$$\text{Population} = \begin{bmatrix} X_1 \\ X_2 \\ \cdots \\ X_{N_{\text{Bat}}} \end{bmatrix}_{N_{\text{Bat}} \times n \times (1+3T)} \tag{67}$$

At the beginning, the first bat of the population is randomly generated from [0, 1]. For the rest of population members, the following equation is used [41]:

$$\mathbf{X}_m = \mu \times \mathbf{X}_{m-1} \times (1 - \mathbf{X}_{m-1}) m = 2, \ldots, N_{\text{Bat}} \tag{68}$$

where, μ displays a control parameter between [0, 4]. Equation (68) has no stochastic pattern in the value of μ and indicates chaotic dynamic when $\mu = 4$[41].

Step 4: Calculating the objective functions. In this way, 2m + 1 Deterministic Load Flow (DLF) is solved corresponding to each member of the population and time interval of the next day and the output variables vector $Z_i(l,k)$is computed. Therefore, the Mean and SD of all the objective functions are determined according to Equation (44).

Step 4 will be repeated for all individuals of the initial population and all time intervals, and the objective function will be calculated using Equations (22)–(26).

Step 5: Storing non-dominated solutions in repository.

Step 6: Updating $\mathbf{Pbest}_m^k$ and $\mathbf{Gbest}^k$: In iteration k, the non-dominated solution of which the value of Equation (47) is maximum, is selected as the best compromise solution ($\mathbf{Gbest}^k$).

At the beginning, the initial produced population is assumed as $\mathbf{Pbest}_m^k$. It is updated provided that one of the following conditions is satisfied; otherwise it is not updated. (1) If the current population dominates former $\mathbf{Pbest}_m^{k-1}$, it is considered as local best. (2) If none of them dominates the other one, the solution of which normalized membership function is greater, is considered as $\mathbf{Pbest}_m^k$.

Step 7: Bats positions modification: The position and velocity of each bat is updated using Equations (52)–(57).

Step 8: Using SALM: ath strategy is selected by RWM as described in Section 9.2 for all existing solution.

Step 9: Comparing the fitness function: Fuzzy membership values of current individuals are compared with those of the previous ones and the better individuals are selected to contribute in the next step using Equation (51).

Step 10: Implementing the 2m + 1 PEM scheme as step 2.

Step 11: Updating the repository by checking out the non-domination.

Step 12: Updating the probability of each mutation strategy i.e. $\text{Prob}_a^k; a = 1, \ldots, 4$ employing Equations (62) and (63).

Step 13: Checking out the convergence criteria: If the current iteration number reaches to a predetermined maximum iteration number, the algorithm is stopped, otherwise go to step 4.

11. Simulation results

In this section, the results of implementing this method in a 69-bus distribution network for planning the location and operation of MCFCPPs as CHPH are represented. The single diagram of this network is shown in Fig. 3. Total nominal load of system is

Table 5
Simulation results of single-objective probabilistic problem for strategy 3.

		Cost function			Emission function			Voltage deviation function		
		Base load	Up load	Low load	Base load	Up load	Low load	Base load	Up load	Low load
Location	$MCFCPP_1$		49			63			18	
	$MCFCPP_2$		61			64			25	
	$MCFCPP_3$		50			62			21	
	$MCFCPP_4$		12			61			23	
P_{MCFCPP}(Kw)	$MCFCPP_1$	401.521	535.5039	2.4845	1.6941×10^3	1.7072×10^3	1.623×10^3	1.6083×10^3	1.1372×10^3	1.483×10^3
	$MCFCPP_2$	1.1896×10^3	1.5166×10^3	787.8012	1.6618×10^3	1.7072×10^3	1.7072×10^3	1.7072×10^3	1.7066×10^3	767.9498
	$MCFCPP_3$	4.998	37.532	2.448	1.7072×10^3	1.7065×10^3	1.6759×10^3	1.6946×10^3	1.7038×10^3	1.7072×10^3
	$MCFCPP_4$	104.541	449.8976	2.448	1.7072×10^3	1.7011×10^3	1.7072×10^3	1.6839×10^3	1.5293×10^3	1.6084×10^3
P_{th}(Kw)	$MCFCPP_1$	1.5152×10^3	1.8423×10^3	1.9736×10^3	2.008×10^3	2.0112×10^3	2.0114×10^3	1.9237×10^3	1.6131×10^3	2.0117×10^3
	$MCFCPP_2$	2.0124×10^3	2.0116×10^3	2.0112×10^3	2.0001×10^3	1.9906×10^3	2.0112×10^3	1.9739×10^3	1.9748×10^3	1.5754×10^3
	$MCFCPP_3$	1.4988×10^3	1.343*103	329.8862	2.0112×10^3	2.0112×10^3	2.0112×10^3	1.9421×10^3	2.007×10^3	1.7194×10^3
	$MCFCPP_4$	1.2775×10^3	629.798	851.1598	2.0112×10^3	2.0112×10^3	2.0001×10^3	2.0112×10^3	1.9712×10^3	1.8261×10^3
$P_{H_{MCFCPP}}$(Kw)	$MCFCPP_1$	1.1035×10^3	1.2944×10^3	1.9579×10^3	300.45	290.4669	374.9371	302.5167	465.0562	515.2338
	$MCFCPP_2$	809.2463	481.6085	1.21×10^3	324.9562	270.0483	290.4669	253.4169	255.0458	796.9268
	$MCFCPP_3$	1.4838×10^3	1.2965×10^3	325.228	290.4669	291.1447	321.838	234.502	289.7474	0.7161
	$MCFCPP_4$	1.1644×10^3	175.6807	843.009	290.4669	296.5947	279.4536	313.8741	428.7064	205.3845
$P_{H_{MCFCPPUsage}}$ (Kw)	$MCFCPP_1$	0	0	0.2445	280.3037	290.4669	374.9371	28.3921	246.0058	511.2513
	$MCFCPP_2$	79.2501	104.6066	0	305.6007	274.9336	289.363	231.3254	162.1566	23.3989
	$MCFCPP_3$	0.0386	8.0232	273.3203	272.4978	283.8361	321.838	190.8137	132.5337	5.5876
	$MCFCPP_4$	36.5213	29.1707	70.4745	120.3503	296.5947	290.4669	298.1804	391.5307	220.368
$P_{H_{Save,MCFCPP}}$ (Kw)	$MCFCPP_1$		4.3556×10^3			2.1428			497.1576	
	$MCFCPP_2$		2.3169×10^3			15.5741			888.5113	
	$MCFCPP_3$		2.8241×10^3			25.2776			196.0305	
	$MCFCPP_4$		2.0469×10^3			159.1033			37.8859	
Function value			6.3899×10^3 $			7.5233×10^7 gr			0.3829 pu	
SD			134.164			4.8367×10^5			0.0013	

Table 6
Comparison of the results obtained by different algorithms considering single-objective probabilistic problem for 100 trials.

Objective function	Algorithm	Best solution	Mean solution	Worst solution	SD	No. of global solution	CPU time (s)
Cost ($)	SALBA	6.3899×10^3	6.39×10^3	6.4172×10^3	6.516	94	170.3
	BA	6.4712×10^3	6.49×10^3	6.5849×10^3	44.829	81	179.7
	PSO	6.5784×10^3	6.61×10^3	6.6914×10^3	49.815	74	192.8
	GA	6.7357×10^3	6.8×10^3	6.9238×10^3	90.743	64	238.4
Emission (gr)	SALBA	7.5233×10^7	7.53×10^7	7.5914×10^7	1.49×10^5	95	122.3
	BA	7.7384×10^7	7.76×10^7	7.8782×10^7	5.28×10^5	83	131.9
	PSO	7.9015×10^7	7.96×10^7	8.1134×10^7	9.66×10^5	71	143.8
	GA	7.9438×10^7	8.03×10^7	8.1928×10^7	11.77×10^5	67	168.2
Voltage deviation (pu)	SALBA	0.3829	0.383	0.3972	0.0028	96	120.9
	BA	0.3922	0.396	0.4118	0.0079	80	130.7
	PSO	0.4015	0.412	0.4473	0.0197	76	138.9
	GA	0.4278	0.451	0.4891	0.0299	62	172.2

considered to be 3802 KW. The base values of voltage and power equal 12.66 KV and 10 MVA respectively. The system data are according to Table 1 [22,24]. The thermal load of every feeder is considered to be 0.4 times of its electrical load. The price values of gas purchasing, hydrogen selling, and the parameters of cost objective function are shown in Table 2 [24,25]. The emission coefficients of NO_x, SO_2, and CO_2 for network and MCFCPPs are represented in Table 3 [42]. Three intervals of operation are considered and the daily load variation is shown in Fig. 4. The uncertainties of electrical and thermal loads forecasting, the pressure of oxygen, hydrogen, and carbon dioxide related to MCFCPP, and operational temperature of MCFCPP are modeled using normal distribution functions.

The location and operation of four 250 KW MCFCPPs are planned in this paper. Since MCFCPPs produce electricity and heat simultaneously, three strategies are considered for investigating the effect of hydrogen production and its recovery by MCFCPP as follows:

Strategy 1: The effect of hydrogen production and recovery is not considered.

Strategy 2: The amount of produced hydrogen equals the difference of MCFCPP maximum capacity and its production power in every load level.

Strategy 3: The amount of hydrogen production varies between zero and the difference of MCFCPP maximum capacity and its production power in every load level.

First, the problem is solved as a multi-objective deterministic problem considering mentioned strategies and its results are brought in Table 4. The produced electrical and thermal power amounts, the equivalent electrical energy of hydrogen importing to storage, and the equivalent electrical energy of consumed hydrogen are shown for each MCFCPP in every load level. The equivalent electrical energy of hydrogen stored in storage which is sold at the end of the day is also brought in this table. The amount of objective function is represented at the bottom of this table. The Pareto curves produced by this simulation method are shown in Figs. 5–7 for three mentioned strategies. The red stars correspond to the best compromise solution considering $i = 1,2,3$ and $w_i = 0.33$ in Equation (47).

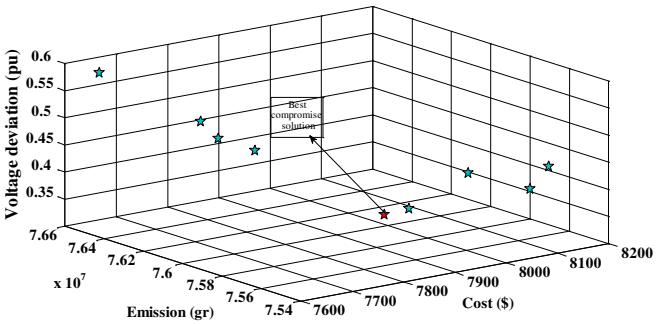

Fig. 9. Pareto front of 2m + 1 PEM for objective functions considering strategy 2.

As illustrated in Table 4, the amount of cost objective function for second strategy is greater than those of the other two strategies. Since MCFCPPs are totally expensive and have low environmentally pollution, using them increases cost, reduces emission, and is effective in reducing voltage deviation. In first strategy, low capacity of MCFCPPs is employed; so, the value of its cost function is lower and those of its emission and voltage deviation function are higher in comparison with strategies 2 and 3. In third strategy, optimal capacities of MCFCPPs are used and the amounts of three objective functions are between those of first and second strategies. In this strategy, the location and operation of MCFCPPs are planned such that all three objective functions are optimally satisfied.

In continue, mentioned uncertainties are considered using 2m + 1 PEM. In this way, at the beginning, the problem is solved as

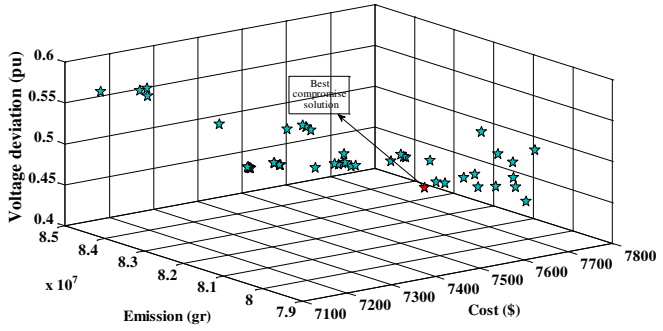

Fig. 8. Pareto front of 2m + 1 PEM for objective functions considering strategy 1.

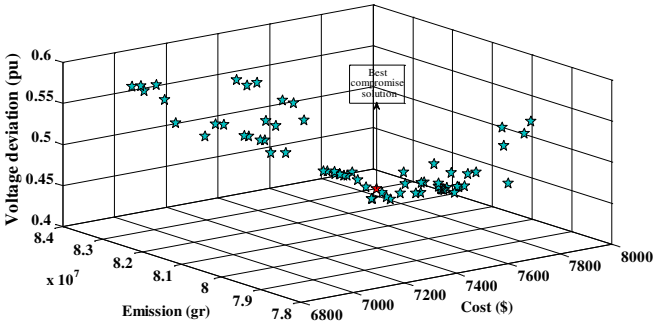

Fig. 10. Pareto front of 2m + 1 PEM for objective functions considering strategy 3.

Table 7
Simulation results of multi-objective probabilistic problem for different strategies.

		Strategy 1			Strategy 2			Strategy 3		
		Base load	Up load	Low load	Base load	Up load	Low load	Base load	Up load	Low load
Location	$MCFCPP_1$		18			64			21	
	$MCFCPP_2$		61			19			58	
	$MCFCPP_3$		21			17			63	
	$MCFCPP_4$		69			61			61	
P_{MCFCPP}(Kw)	$MCFCPP_1$	1.639×10^3	1.6949×10^3	1.7072×10^3	1.517×10^3	825.5763	1.4156×10^3	1.5975×10^3	1.7072×10^3	1.5868×10^3
	$MCFCPP_2$	1.5902×10^3	539.1645	1.6407×10^3	1.0218×10^3	197.9351	1.6055×10^3	2.448	61.5972	1.7072×10^3
	$MCFCPP_3$	1.6582×10^3	1.4651×10^3	1.7072×10^3	909.3276	1.5638×10^3	1.2452×10^3	1.4839×10^3	1.7072×10^3	470.1153
	$MCFCPP_4$	509.8463	1.4771×10^3	1.1178×10^3	969.244	1.018×10^3	870.1828	1.7042×10^3	1.7072×10^3	533.8333
P_{th}(Kw)	$MCFCPP_1$	1.6501×10^3	1.7064×10^3	1.7187×10^3	2.0135×10^3	2.0135×10^3	2.0135×10^3	1.68×10^3	1.9927×10^3	1.9*103
	$MCFCPP_2$	1.6009×10^3	542.8013	1.6517×10^3	2.0135×10^3	2.0135×10^3	2.0135×10^3	960.4856	1.8213×10^3	1.7597×10^3
	$MCFCPP_3$	1.6694×10^3	1.475×10^3	1.7187×10^3	2.0135×10^3	2.0135×10^3	2.0135×10^3	1.9058×10^3	1.7266×10^3	1.4109×10^3
	$MCFCPP_4$	513.2853	1.4871×10^3	1.1253×10^3	2.0135×10^3	2.0135×10^3	2.0135×10^3	1.9632×10^3	2.0112×10^3	1.0643×10^3
$P_{H_{MCFCPP}}$(Kw)	$MCFCPP_1$	0	0	0	483.0393	1.1744×10^3	584.3704	71.2359	272.0897	300.4148
	$MCFCPP_2$	0	0	0	978.2445	1.8021×10^3	393.4537	951.6023	1.7475×10^3	40.7241
	$MCFCPP_3$	0	0	0	1.0907×10^3	436.1884	754.7726	409.1408	7.8277	931.3314
	$MCFCPP_4$	0	0	0	1.0308×10^3	981.9884	1.1298×10^3	245.8931	290.4669	523.3177
$P_{H_{MCFCPPUsage}}$ (Kw)	$MCFCPP_1$	0	0	0	483.0393	1.1744×10^3	584.3704	0	0	319.0284
	$MCFCPP_2$	0	0	0	978.2445	1.8021×10^3	393.4537	224.6143	23.3411	278.0115
	$MCFCPP_3$	0	0	0	1.0907×10^3	436.1884	754.7726	92.5794	247.3209	277.6912
	$MCFCPP_4$	0	0	0	1.0308×10^3	981.9884	1.1298×10^3	231.136	18.4705	288.3348
$P_{H_{Save,MCFCPP}}$ (Kw)	$MCFCPP_1$		0			0			324.712	
	$MCFCPP_2$		0			0			2.2139×10^3	
	$MCFCPP_3$		0			0			730.7083	
	$MCFCPP_4$		0			0			521.7364	
Cost ($)	Value		7.495×10^3			7.8441×10^3			7.3771×10^3	
	SD		20.693			20.883			20.7601	
Emission (gr)	Value		8.0334×10^7			7.5613×10^7			7.9855×10^7	
	SD		4.8219×10^5			4.8112×10^5			4.8283×10^5	
Voltage Deviation (pu)	Value		0.4783			0.3912			0.4753	
	SD		0.0021			0.0021			0.0022	

a probabilistic single-objective one and obtained results are illustrated in Table 5. Investigation of this table shows that in case of considering cost as objective function $P_{H_{MCFCPPUsage}}$ is less than those of the other objective functions and $P_{H_{Save,MCFCPP}}$ of this case is also higher than those of the others. Since MCFCPPs are expensive, if cost objective function is the sole objective function, low capacities of MCFCPPs are employed; but when emission or voltage deviation is considered as objective function, larger capacities of MCFCPPs are employed because MCFCPPs are very effective in reduction of these two objective functions.

The results of different algorithms for third strategy and also those of three single objectives are shown in Table 6. According to these results, proposed method obtains smaller values in comparison with other algorithms. The convergence times out of 100 times of executing the program related to SALBA is more than those of others which confirms its robustness. Results show that CPU time of SALBA is less than that of BA and it converges to optimum solution in lower iterations.

In continue, the problem is considered to be multi-objective considering mentioned uncertainties using $2m + 1$ PEM. The Pareto curves related to the different strategies are illustrated in Figs. 8–10. The best compromise solution, considering $i = 1,2,3$ and $w_i = 0.33$ in Equation (47), are discriminated by red stars and the results are shown in Table 7. According to the results of this table,

Table 8
Comparison of the results obtained by different algorithms considering multi-objective probabilistic problem for 100 trials.

		Algorithm			
		SALBA	BA	PSO	GA
Average solution	Cost ($)	7.3771×10^3	7.4952×10^3	7.5814×10^3	7.8236×10^3
	Emission (gr)	7.9855×10^7	8.0247×10^7	8.1527×10^7	7.2642×10^7
	Voltage deviation (pu)	0.4753	0.4759	0.4867	0.5038
	N_μ	0.0188	0.0172	0.0154	0.0138
Average solution	Cost ($)	7.38×10^3	7.49×10^3	7.64×10^3	7.87×10^3
	Emission (gr)	7.99×10^7	8.04×10^7	8.17×10^7	8.25×10^7
	Voltage deviation (pu)	0.475	0.476	0.486	0.514
	N_μ	0.0187	0.017	0.0151	0.0132
Worst solution	Cost ($)	7.3645×10^3	7.4714×10^3	7.8114×10^3	7.9437×10^3
	Emission (gr)	8.0038×10^7	8.1052×10^7	8.2173×10^7	8.2217×10^7
	Voltage deviation (pu)	0.4756	0.4798	0.4824	0.5314
	N_μ	0.0171	0.0158	0.0141	0.0123
	SD	0.000406	0.000473	0.000566	0.000732
	No. global solution	94	87	75	62
	CPU time (s)	410.9	522.7	630.8	652.9

the thermal energy production of MCFCPPs of first strategy is less than those of strategies 2 and 3 because the equivalent energy of hydrogen recovery is not considered in this strategy; while it is considered in strategies 2 and 3 and this consideration causes to some extent in heat generation. In strategy 2, $P_{H_{Save.MCFCPP}}$ of all the four MCFCPPs is zero because whole the $P_{H_{MCFCPP}}$ entering the storage is used in this strategy and no hydrogen remains in storage at the end of operation duration. The results of this table show that strategy 3 presents an optimal state of hydrogen usage. The least values of voltage deviation and emission functions relate to strategy 2 because the maximum capacity of MCFCPPs is employed in this strategy.

According to Equation (34), the overall efficiency of $MCFCPP_1$ equals 69%, 79%, and 75% for strategies 1, 2, and 3 respectively. The overall efficiency of strategy 1 is the least because the effect of hydrogen production is not considered in it. The best overall efficiency relates to strategy 2 in which the maximum amount of hydrogen is used. The overall efficiency of strategy 3 as an optimal state is between those of the other two strategies.

The results of the proposed algorithm and those of the other algorithm are compared in Table 8 considering a probabilistic multi-objective problem. As illustrated, the results of SALBA dominate the results of other algorithms very well. Also the SD obtained for N_μ is smaller than those of the others. The CPU time of SALBA is lower and its number of convergence to global optima out of 100 times of program execution is higher than those of other algorithms.

Each solution of Pareto optimal set could be an acceptable solution for decision maker and one of them could be selected by decision maker as the best compromise solution according to the importance of each objective function. After producing Pareto optimal set by SALBA, using Equation (47), a normalized membership function is added to this set for selecting the best compromise solution. In this method, importance rates of objective functions should be determined. In this way w_i is considered to be the importance coefficient of objective function. In this paper, w_1, w_2, and w_3 relate to the importance degree of cost, emission, and voltage deviation respectively. For better explanation of the problem, four cases are studied in this paper considering strategy 3:

Case I: Considering a probabilistic cost function.

Case II: Considering a probabilistic emission function.

Case III: Considering a probabilistic voltage deviation function.

Case IV: Considering a probabilistic multi-objective function,

The results of exerting fuzzy decision making approach on Pareto optimal set are shown in Table 9. Following results can be concluded using the investigation of this table:

- In cases I–III when an objective function is minimized as a single-objective function, its value is the least and the values of the other two objective functions increase in comparison with their minimum values.
- The function of cost and emission are in conflict. For example in case IV, when $w_1 = 0.8$ and $w_2 = 0.1$, cost and emission are 6.4955×10^3 \$ and 8.3194×10^7 gr respectively. On the other hand when $w_1 = 0.1$ and $w_2 = 0.8$ cost and emission functions equal 7.7811×10^3 \$ and 7.8762×10^7 gr. The results of cases I and II confirm the mentioned claim.
- The functions of cost and voltage deviation are in conflict. MCFCPPs should produce more active power for minimizing voltage deviation. Since producing energy by MCFCPPs is expensive, cost increases. The results of cases I, III, and IV validate above mentioned facts.
- Objective functions of emission and voltage deviation behave similarly. In case IV-2, 3, when w_3 remains constant and w_2 increases, the value of voltage deviation objective function reduces.
- Case IV-1 presents a compromise between all objective functions.

Table 9
Fuzzy decision making on Pareto optimal set.

Cases	Importance			Cost ($)	Emission (gr)	Voltage deviation (pu)
	w1	*w2*	*w3*			
Case I	–	–	–	6.3899×10^3	8.6293×10^7	0.5895
Case II	–	–	–	7.6713×10^3	7.5233×10^7	0.4399
Case III	–	–	–	7.903×10^3	7.8649×10^7	**0.3829**
Case IV	0.33	0.33	0.33	7.3771×10^3	7.9855×10^7	0.4753
	0.8	0.1	0.1	6.4955×10^3	8.3194×10^7	0.5742
	0.1	0.8	0.1	7.7811×10^3	7.8762×10^7	0.5356
	0.1	0.1	0.8	7.4963×10^3	8.0735×10^7	0.4427

12. Conclusions

The location and operation of MCFCPPs are planned using SALBA considering a multi-objective function. Total operation cost of network and MCFCPPs, total emission of network and MCFCPPs, and total voltage deviation of buses from nominal values are the objective functions considered in this paper. The Pareto optimization method is employed to solve the multi-objective problem and finally a set of solutions called Pareto optimal set is presented. That this method enables the decision maker to consider importance coefficients of objective functions and his/her personal experiences for selecting the best compromise solution, is one of the advantages of this method. The convergence characteristics are noticeably improved using a self adaptive mutation technique. MCFCPPs are operated for producing heat, electrical power, and hydrogen simultaneously. Operation of MCFCPPs as CHPH increases the operational efficiency and has many benefits for system operator. In this paper, the uncertainties of electrical and thermal loads, pressure of oxygen, hydrogen, and carbon dioxide importing to MCFCPP, and operational temperature of MCFCPP are considered using $2m + 1$ PEM which results in more reliable operation of network. Totally an effective algorithm with low convergence time is proposed in this paper for optimal planning of location and operation of MCFCPPs employed as CHPH. The simulation results validate the effective and favorable performance of the suggested method.

References

[1] V. Chiodo, F. Urbani, A. Galvagno, N. Mondello, S. Freni, J. Power Sources 206 (2012) 215–221.
[2] T. Niknam, A. Kavousifard, S. Tabatabaei, J. Aghaei, J. Power Sources 196 (2011) 8881–8896.
[3] H. Jeong, S. Cho, D. Kim, H. Pyun, D. Ha, C. Han, M., Kang, M. Jeong, S. Lee, Int. J. Hydrogen Energy 37 (2012) 11394–11400.
[4] D.W. Hengeveld, S.T. Revankar, J. Power Sources 165 (2007) 300–306.
[5] U. Desideri, S. Proietti, P. Sdringola, G. Cinti, F. Curbis, Int. J. Hydrogen Energy xxx (2012) 1–9.
[6] M.C. Williams, H.C. Maru, J. Power Sources 160 (2006) 863–867.
[7] J.J. Hwang, J. Power Sources 223 (2013) 325–335.
[8] M. Nayeripour, M. Hoseintabar, T. Niknam, J. Power Sources 196 (2011) 4033–4043.
[9] R.S. Al Abri, E.F. El-Saadany, Y.M. Atwa, IEEE Trans. Power Syst. (2012) 1–9.
[10] Z. Moravej, A. Akhlaghi, Electr Power Energy Syst. 44 (2013) 672–679.
[11] S. Biswas, S.K. Goswami, A. Chatterjee, Energy Convers. Manage. 53 (2012) 163–174.
[12] Sh. Abdi, K. Afshar, Electr Power Energy Syst. 44 (2013) 786–797.
[13] A.M. El-Zonkoly, IET Gener Transm. Dis. 5 (2011) 760–771.
[14] Q. Kang, T. Lan, Y. Yan, L. Wang, Q. Wu, Neurocomputing 78 (2012) 55–63.
[15] M.H. Moradi, M. Abedini, Electr Power Energy Syst. 34 (2012) 66–74.
[16] T. Niknam, S.I. Taheri, J. Aghaei, S. Tabatabaei, M. Nayeripour, Appl. Energy 88 (2011) 4817–4830.
[17] R.A. Jabr, B.C. Pal, IET Gener Transm. Dis. 3 (2009) 713–723.
[18] M.R. AlRashidi, M.F. AlHajri, Energy Convers. Manage. 52 (2011) 3301–3308.
[19] L. Wang, C. Singh, IEEE Trans. Power Syst. 38 (2008) 757–764.

[20] H. Hedayati, S.A. Nabaviniaki, A. Akbarimajd, IEEE Trans. Power Delivery. 23 (2008) 1620–1628.
[21] R. Rashidi, I. Dincer, P. Berg, J. Power Sources 185 (2008) 1107–1114.
[22] R. Rashidi, P. Berg, I. Dincer, Int. J. Hydrogen Energy 34 (2009) 4395–4405.
[23] T. Niknam, F. Golestaneh, A.R. Malekpour, J. Power Sources 229 (2013) 285–298.
[24] M.Y. El-Sharkh, M. Tanrioven, A. Rahman, M.S. Alam, J. Power Sources 153 (2006) 136–144.
[25] M.Y. El-Sharkh, M. Tanrioven, A. Rahman, M.S. Alam, J. Power Sources 161 (2006) 1198–1207.
[26] E. Farjah, M. Bornapour, T. Niknam, B. Bahmanifirouzi, Energies 5 (2012) 790–814.
[27] S. Ahmed, D.D. Papadias, R.K. Ahluwalia, Configuring a fuel cell based residential combined heat and power system, J. Power Sources, Accepted Manuscript xxx (2013) xxx–xxx, in press.
[28] M. Hosseini, I. Dincer, M.A. Rosen, J. Power Sources 221 (2013) 372–380.
[29] S. Wongchanapai, H. Iwai, M. Saito, H. Yoshida, J. Power Sources 223 (2013) 9–17.
[30] R.Y. Rubinstein, Simulation and the Monte Carlo Method, Wiley, New York, 1981.
[31] A.R. Malekpour, T. Niknam, Energy 36 (2011) 3477–3488.
[32] J.M. Morales, J. Perez-Ruiz, IEEE Trans. Power Syst. 22 (2007) 1594–1601.
[33] T.C. Bora, L.D.S. Coelho, L. Lebensztajn, IEEE Trans. Magn. 48 (2012) 947–950.
[34] A.L. Dicks, Curr. Opin. Solid State Mater. Sci. 8 (2004) 379–383.
[35] J.H. Koh, B.S. Kang, H.C. Lim, J. Power Sources 91 (2000) 161–171.
[36] C.Y. Yuh, J.R. Selman, J. Electrochem. Soc. 138 (1991) 3642–3648.
[37] O. Grillo, L. Magistri, A.F. Massardo, J. Power Sources 115 (2003) 252–267.
[38] T. Niknam, E. Azad Farsani, M. Nayeripour, B. Bahmani Firouzi, Eur. Trans. Electr. Power 20 (2011) 1–26.
[39] X.S. Yang, A New Metaheuristic Bat-Inspired Algorithm, Nature Inspired Cooperative Strategies for Optimization (NICSO 2010) vol. 284, Springer, 2010, pp. 65–74. Studies Computational Intelligence.
[40] C.K. Panigrahi, P.K. Chattopadhyay, R.N. Chakrabarti, M. Basu, Electr Power Compon Syst. 34 (2006) 577–586.
[41] R. Caponetto, L. Fortuna, S. Fazzino, M.G. Xibilia, IEEE Trans. Evol. Comput. 7 (2003) 289–304.
[42] ERDC-CERL Fuel Cell Website, http://dodfuelcell.cecer.army.mil/library_items/RIA_MCFC.pdf.